Retinal Nerve Fiber Layer Protrusion Associated with Tilted Optic Discs

Jaclyn Chiang, MOptom,[1,2] Michael Yapp, MOptom, FAAO,[1,2] Angelica Ly, BOptom, FAAO,[1,2]
Michael P. Hennessy, MBiomedE, MBBS,[1,3] Michael Kalloniatis, PhD, MScOptom, FAAO,[1,2] and Barbara Zangerl, PhD, DVM[1,2]*

SIGNIFICANCE: This study resulted in the identification of an optic nerve head (ONH) feature associated with tilted optic discs, which might potentially contribute to ONH pathologies. Knowledge of such findings will enhance clinical insights and drive future opportunities to understand disease processes related to tilted optic discs.

PURPOSE: The aim of this study was to identify novel retinal nerve fiber layer (RNFL) anomalies by evaluating tilted optic discs using optical coherence tomography. An observed retinal nerve fiber protrusion was further investigated for association with other morphological or functional parameters.

METHODS: A retrospective review of 400 randomly selected adult patients with ONH examinations was conducted in a referral-only, diagnostic imaging center. After excluding other ONH pathologies, 215 patients were enrolled and evaluated for optic disc tilt and/or torsion. Gross anatomical ONH features, including size and rim or parapapillary region elevation, were assessed with stereoscopic fundus photography. Optical coherence tomography provided detailed morphological information of individual retinal layers. Statistical analysis was applied to identify significant changes between individual patient cohorts.

RESULTS: A dome-shaped hyperreflective RNFL bulge, protruding into the neurosensory retina at the optic disc margins, was identified in 17 eyes with tilted optic discs. Available follow-up data were inconclusive regarding natural changes with this ONH feature. This RNFL herniation was significantly correlated with smaller than average optic disc size ($P = .005$), congenital disc tilt ($P < .0001$), and areas of rim or parapapillary elevation ($P < .0001$).

CONCLUSIONS: This study reports an RNFL protrusion associated with tilted optic discs, which has not previously been assessed as an independent ONH structure. The feature is predominantly related to congenital crowded, small optic discs and variable between patients. This study is an important first step to elucidate diagnostic capabilities of tilted disc morphological changes and understanding associated functional deficits.

Optom Vis Sci 2018;95:239–246. doi:10.1097/OPX.0000000000001179

Supplemental Digital Content: *Direct URL links are provided within the text.*

SDC OPEN

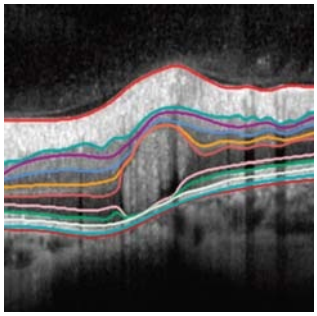

Author Affiliations:
[1]Centre for Eye Health, University of New South Wales, Kensington, New South Wales, Australia
[2]School of Optometry and Vision Science, University of New South Wales, Kensington, New South Wales, Australia
[3]Ophthalmology, Prince of Wales Hospital, Randwick, New South Wales, Australia
*bzangerl@cfeh.com.au

Tilted optic discs, classified according to their etiology as either congenital or acquired, occur in the general population at a prevalence of 0.4 to 3.5% with bilateral presentation in 37.5 to 80% of cases.[1–3] The congenitally tilted optic disc is a nonprogressive condition associated with incomplete closure of the embryonic fissure resulting in the optic nerve appearing to enter the eye at an oblique angle while also showing optic disc torsion.[2–4] The tilt most frequently occurs in the inferonasal direction with an elevated and indistinct disc margin at the corresponding superotemporal aspect.[2] In contrast, an acquired tilted optic disc arises due to changes associated with high myopia and is considered progressive.[5] Although it has been established that congenitally tilted optic discs are more frequently observed in myopic and astigmatic eyes,[1,3,6,7] and possibly predict myopic progression rates,[8] not all high myopes exhibit this feature.[9]

It may not always be possible to distinguish between congenitally and acquired tilted optic discs[2]; the tilt itself, however, can be described using characterizing features, such as the index of tilt, degree of torsion,[3,10,11] and/or edge protrusion of the optic disc.[12,13] Recent findings in tilted optic discs include the protrusion of the upper edge of Bruch's membrane and choroid accompanied by a herniation and bending of the nerve tissue into this protrusion in adult tilted disc syndromes.[13] Another compelling study described a dome-shaped hyperreflective bulge protruding from Bruch's membrane and choroid in the form of a retinal nerve fiber layer herniation-like structure in pediatric patients.[12] Almost half the pediatric subjects with this herniation presented with visual field defects proposed as a direct consequence of the herniation and bending of the nerve fibers superiorly.[12] An identical-looking structure was described by Kulkarni et al.[14] in some patients suffering from optic nerve head drusen. We therefore hypothesized that retinal nerve fiber layer irregularities are a common feature in adult tilted optic discs and contribute to functional deficits.

While optical coherence tomography is used extensively for optic nerve head imaging with a focus on retinal nerve fiber layer thickness,[15–19] analyses of morphological changes in tilted discs are limited.[20] We used high-resolution spectral domain optical coherence tomography *in vivo* imaging of the optic disc and visualization of parapapillary retinal architecture to assist in the systematic, morphological analysis of tilted optic discs.

METHODS

Selection Criteria

Written consent was obtained from 400 randomly chosen patients referred to the Centre for Eye Health (CFEH) for optic nerve head or glaucoma assessment over a period of 3 years (2013–2015) in accordance with the Declaration of Helsinki and approved by the Biomedical Human Research Ethics Advisory Panel of UNSW Australia. More than 6000 patients were seen during this time, 87% of whom were excluded due to the presence of optic disc pathology other than tilting, such as optic disc pits or glaucoma, known neurological pathology potentially leading to retrograde degeneration, and poor optical coherence tomography image quality (<7/10 signal strength). Patients included in the current study further had to be older than 18 years and have high-quality stereoscopic optic disc images defined as free of artifacts, in focus, and with adequate contrast and brightness. A random-number generator was applied to approximately 700 patients potentially eligible for this study, and the first 400 were selected for further review. As CFEH serves as a referral-only imaging and diagnostic center, patients are typically managed by the primary referrer. Therefore, follow-up data cannot always be obtained, specifically if patients move or change their primary eye health care provider. Follow-up data were collected for patients included in this research, where available, subsequent to the initial diagnosis to prevent biases.

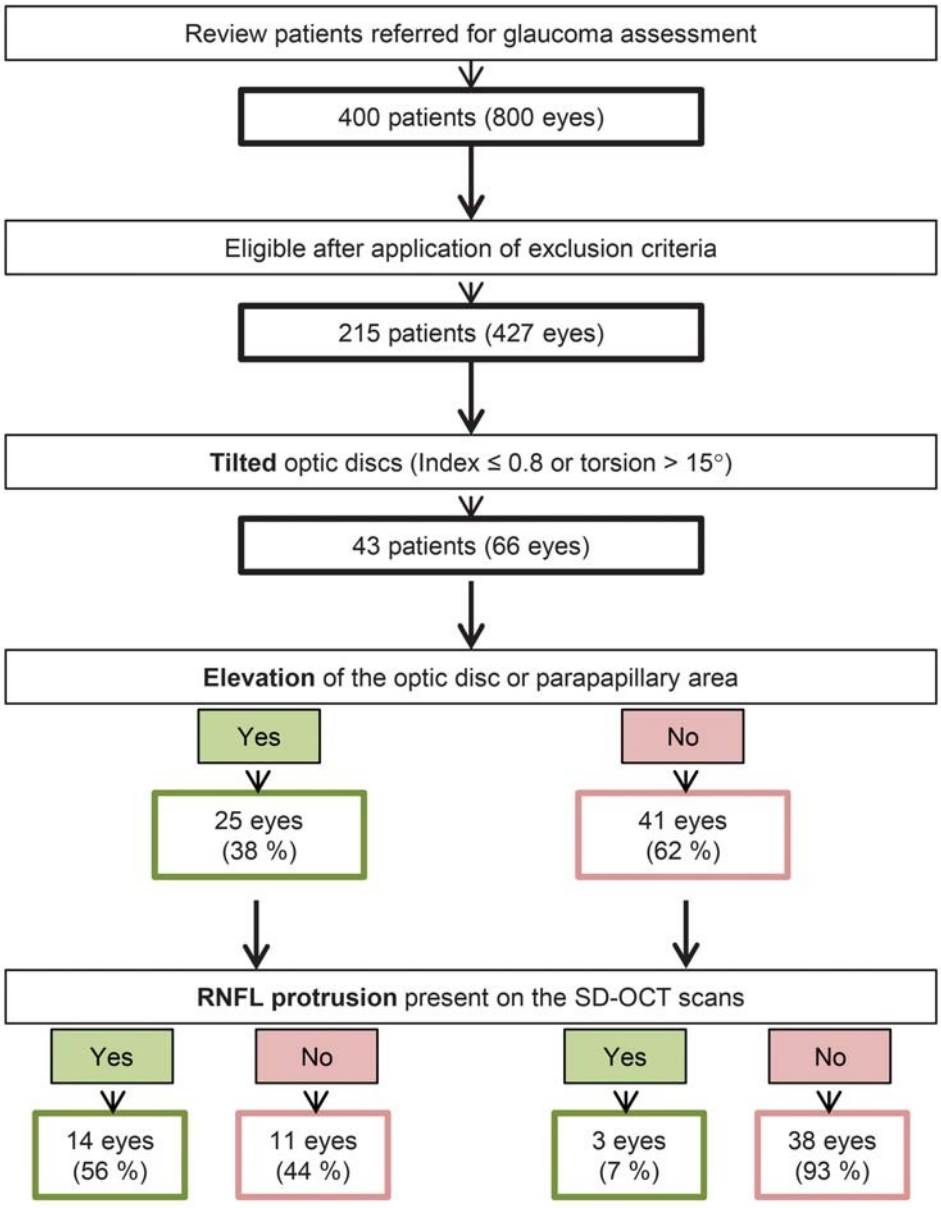

FIGURE 1. Workflow and main classifications. Of 400 randomly selected patients (800 eyes) referred for optic nerve head assessment, 215 (407 eyes) were eligible for the current study identifying 43 patients (66 eyes) with tilted optic discs. Investigated structural criteria revealed elevation of the optic disc or parapapillary area in 25 and 17 eyes with retinal nerve fiber layer protrusion. A strong association between optic disc or parapapillary elevation and RNFL protrusion was observed (n = 45, $\chi^2 = 12.8$, $P = .0003$).

TABLE 1. Patient characteristics

Patients (n)	Eligible (215)	Nontilted (172)	Tilted (43)	*P*
Age (y)				
Mean (SD)	55.7 ± 15.1	57.8 ± 13.8	47.1 ± 17.1	<.001
Range	20 to 89	20 to 89	20 to 76	
Sex, n (%)				
M	115 (53.5)	101 (58.7)	14 (32.6)	.002
F	100 (46.5)	71 (41.3)	29 (67.4)	.002
Total eyes (n)	**407**	**341**	**66**	
Spherical equivalent				
Median	–0.38	–0.13	–1.88	<.001
Range	–10.75 to 7.63	–10.50 to 7.63	–10.75 to 2.75	
Myopic eyes, n (%)				
–1 to –6 D	153 (37.6)	112 (32.8)	41 (62.1)	<.001
≤–6 D	19 (4.7)	10 (2.9)	9 (13.6)	
Astigmatism, n (%)				
Up to 1 DC	312 (76.7)	270 (79.2)	42 (63.6)	.006
>1 DC	95 (23.3)	71 (20.8)	24 (36.4)	

Two hundred fifteen patients were reviewed and examined for tilted discs. Patients characteristics were compared between tilted and nontilted discs using χ^2 (sex, myopia, astigmatism) or Student *t* test (age, spherical equivalent), and corresponding *P* values support significant differences between cohorts. DC = diopters cylinder; F = female; M = male; n = total number.

Clinical Assessment

Standard assessments included slit-lamp examination, measurement of intraocular pressures, funduscopy, visual field testing, stereoscopic optic disc photography, and spectral domain optical coherence tomography imaging.[21] Stereoscopic optic disc images and posterior pole fundus images were obtained through dilated pupils with a nonmydriatic fundus camera (Kowa nonmyd WX 3D Stereo Fundus Camera; Kowa, Tokyo, Japan). Spectral domain optical coherence tomography images were acquired using the Cirrus optical coherence tomography (Cirrus HD-OCT 4000, version 7.0; Carl Zeiss Meditec, Inc., Dublin, CA) with the optic disc cube 200 × 200 protocol centered on the optic disc, and B-scan cross sections were analyzed with Advanced Visualization. Visual field testing was performed with standard automated perimetry (Humphrey Field Analyzer 750; Zeiss/Humphrey Systems, Dublin, CA) or the Humphrey Matrix Frequency Doubling Technology perimeter (Matrix; Carl Zeiss Meditec, Inc.) according to the referring clinician's specifications. We attempted to obtain visual field results from patients who did not have reliable tests on file but were not always able to recall patients specifically if they were considered healthy and did not remain under clinical management. While optical coherence tomography scans were obtained from all patients, additional high-resolution optical coherence tomography was obtained from selected patients for detailed investigation of findings using the Heidelberg Spectralis OCT (Heidelberg Engineering, Heidelberg, Germany) with 30° ART 97 B-scans at enhanced depth image mode centered around the optic nerve head if clinically indicated.

Data Collection

Age, sex, visual acuity, and refractive error were recorded for all patients. Myopia was defined as a spherical equivalent of greater than –1 diopters (D) and further classified into mild (–1 > –3 D), moderate (–3 > –6 D), or high (≤–6.00 D) myopia. Optic disc size was measured from nonmydriatic fundus photographs obtained with a Kowa WX 3D camera. Disc margins were subjectively defined using stereoscopic optic disc photographs. Assessing the color and contour of the disc surface and blood vessels, optic discs were outlined independently by two observers by positioning a number of anchor points along the disc margin using the Kowa WX 3D Analysis software. The software generates a smooth line connecting these anchor points using closed curve spline interpolation to form a circle, which is adjusted by the observers to form the best fit to the disc margin. Absolute size was calculated using the software after correcting for magnification and axial length using the "Best Fit Sphere" and "Central Corneal Curvature" feature based on the spherical equivalent in diopters provided for each patient. Disc size determination was subsequently verified by an ophthalmologist with a special interest in glaucoma, and the average between the two measurements was used for analysis as all

TABLE 2. Relation between tilt ratio and spherical equivalent based on 66 tilted eyes of 43 patients

	Spherical equivalent (D)			
Tilt ratio, n (%)	**>–1 D no myopia**	**–1 > –3 D mild myopia**	**–3 > –6 D moderate myopia**	**≤–6 D high myopia**
>0.80–0.70, No to moderate tilt	16 (100.0)	16 (76.2)	14 (70.0)	6 (66.7)
<0.70, Severe tilt	0 (0.0)	5 (23.8)	6 (30.0)	3 (33.3)

measurements differed by less than 10%. Tilted discs were identified by an index of tilt of 0.80 or less or degree of torsion of the longest diameter beyond 15 degrees of the vertical meridian.[3,11] The index of tilt was defined as the minimum to maximum disc diameter ratio and classified into less than 0.70 (severe tilt), 0.70 to 0.74 (moderate tilt), 0.75 to 0.80 (mild tilt), and greater than 0.80 (not tilted).[11] For the purpose of this study, discs for which the degree of torsion was greater than 45° and the tilt occurred inferonasally were classified as congenital. Discs were categorized as congenitally crowded if at least two quadrants were elevated with indistinct disc margins in the presence of a small disc (<2.4 mm^2).[6] The remainder was considered acquired tilted discs. Presence and location of elevation at the optic disc or parapapillary area were identified based on stereoscopically viewed funduscopic disc features of an indistinct disc margin (where the upper edge of the optic disc protruded anteriorly relative to its lower edge). All measurements were performed by two independent masked observers and arbitrated by a third masked observer if equivocal.

Potential visual field defects were assessed from initial and reliable tests and confirmed on follow-up fields, where available. Test reliability was defined as less than 20% fixation less and less than 33% false-negative or false-positive errors and deficits were classified with regard to their type and location as described by Keltner et al.[22] Briefly, two masked observers determined whether a localized (temporal wedge, enlarged blind spot, nasal step, paracentral, partial arcuate, arcuate, altitudinal) or diffuse (multiple foci or widespread) visual field defect was present and subsequently specified the location of the most severe depression. For the purpose of this study, quadrantanopia and hemianopia were classified as localized defects. Mean deviation and pattern standard deviation were recorded for all visual field tests and interpreted independently for Humphrey Field Analyzer or Matrix in accordance to the manufacturer's definitions, whereas classification based on the general area of the defect was considered comparable between instruments. In all cases, equivocal results were reviewed by a third observer masked to the patient status and other classifications.

Data Analysis

A χ^2 statistic or Student *t* test was applied to identify statistically significant distributions between individual patient groups using a single eye for each patient. If both eyes of a patient were eligible for the study, one was chosen using a random-number generator.

RESULTS

Occurrence and Features of Tilted Optic Discs

A total of 215 patients passed study exclusion criteria, with another three eyes excluded because of poor image quality. Tilted optic discs were present in 66 eyes of 43 subjects of this cohort (Fig. 1) and associated with female sex ($\chi^2(1) = 9.5$, $P = .002$), astigmatism ($\chi^2(1) = 7.5$, $P = .006$), and myopia ($\chi^2(2) = 41.5$, $P < .0001$) when compared with nontilted discs (Table 1). High myopia was furthermore more frequently observed in optic discs with severe tilt (Table 2). Optic nerve head elevation and visual field results were examined in more detail in those eyes that presented with tilted discs. Elevation of the optic disc or parapapillary area was observed in 25 eyes, predominantly present superiorly (n = 22). More than two thirds of the optic discs demonstrated elevation in more than one quadrant, mostly in the nasal (n = 17) and inferior (n = 10) areas; temporal extension was present in only three eyes (Table 3, Appendix Table A1, http://links.lww.com/OPX/A329).

TABLE 3. Clinical findings for patients with retinal nerve fiber layer (RNFL) protrusion at the optic nerve head

						Optic disc features				Visual field defects		
Patient	Eye	P*	E*	SE	VA	Size (mm^2)	Index of tilt	Torsion (degrees)	R†	Mean deviation	Pattern standard deviation	Defect
1: 19 y, F	**OD**	**S**	**S, N**	**–0.50**	**6/6**	**1.24**	**0.78**	**37**	**H**	**–2.76**	**2.18**	**Widespread**
2: 20 y, M	OD	N	None	–1.88	6/6	2.48	0.80	5	M	–3.39	2.56	Multiple foci
3: 24 y, F	OD	S, T	S, N	+0.50	6/9.5	1.43	0.76	–17	H	–1.11	1.62	Multiple foci
	OS	**S, T**	**S, T**	**+1.75**	**6/9.5**	**1.20**	**0.82**	**–46**	**H**	**–2.25**	**1.71**	**No defect**
4: 27 y, M	**OD**	**N**	**S, N, I**	**–3.25**	**6/6**	**1.23**	**0.75**	**–13**	**H**	**–2.55**	**2.37**	**No defect**
	OS	N	S, N, I	–3.88	6/6	1.42	0.79	22	H	–1.43	1.96	Paracentral, SN
5: 28 y, F	OD	N	S, N	–5.50	$6/6^{-1}$	1.94	0.80	–26	C	–1.59	1.58	Multiple foci
	OS	**N**	**S, N**	**–6.25**	**$6/6^{-1}$**	**1.27**	**0.79**	**–21**	**C**	**–2.64**	**1.96**	**No defect**
6: 30 y, F	OD	S, T	S, T	–1.50	6/6	1.60	0.86	–19	H	0.29	1.43	Paracentral, I
	OS	**S, T**	**S, T**	**–6.63**	**6/6**	**1.72**	**0.73**	**–47**	**H**	**–3.09**	**1.68**	**Paracentral, S**
7: 31 y, F	OD	S, N	S, N	0.00	6/6	1.40	0.73	30	H		Not available	
	OS	**S, N**	**S, N, I**	**0.00**	**6/6**	**1.85**	**0.79**	**13**	**H**		**Not available**	
8: 32 y, F	**OD**	**S, N, I**	**S, N, I**	**–1.88**	**6/9.5**	**1.58**	**0.66**	**–12**	**H**	**0.8‡**	**3.37‡**	**Nasal step**
	OS	S, N, I	S, N, I	–1.88	$6/6^{+2}$	1.44	0.58	–15	H	1.97‡	2.53‡	No defect
9: 60 y, M	OD	N	None	–1.13	6/6	1.16	0.59	–15	M	1.25‡	2.4‡	No defect
	OS	**S, N**	**None**	**–1.88**	**$6/7.6^{+2}$**	**1.06**	**0.60**	**20**	**M**	**–1.01‡**	**4.62‡**	**Quadrant, ST**
10: 70 y, F	**OD**	**S**	**S**	**–0.50**	**$6/12^{+1}$**	**1.07**	**0.78**	**–82**	**C**		**Not available**	

Clinical details for 10 patients (17 eyes) identified with RNFL protrusion (P), including elevation (E) of the optic disc, spherical equivalent (SE) in diopter, visual acuity (VA), and main reason for the observed tilt (R). Eyes in bold font were included in statistical analysis. *Superior (S), inferior (I), temporal (T), or nasal (N) location of feature; †heaped (H), congenital (C), or myopic (M) disc; ‡visual field test was performed on the Humphrey Matrix.

Visual field tests were available in 41 patients (n = 30 and 11 for Humphrey Field Analyzer and Matrix, respectively), and defects were observed in 35 subjects. The majority of defects were localized (n = 27 and 7 for Humphrey Field Analyzer and Matrix, respectively); 14 eyes presented with diffuse visual field loss (n = 12 and 2 for Humphrey Field Analyzer and Matrix, respectively), and total loss of vision was recorded for one eye (Table 3, Appendix Table A1, http://links.lww.com/OPX/A329). The mean deviation within the cohort was –3.0 dB ± 5.2 and –1.1 dB ± 2.7 for Humphrey Field Analyzer (n = 30) and Matrix (n = 11), respectively; pattern standard deviation was 2.2 dB ± 1.0 and 3.4 dB ± 1.0 for the same subgroups.

Presentation of Presumed Retinal Nerve Fiber Layer Protrusion

Close examination of the spectral domain optical coherence tomography serial line scans identified an anomaly in the optic disc architecture visible as a dome-shaped hyperreflective bulge at the margins of the optic disc in the area where the retinal nerve fiber layer changes course to pass through Bruch's membrane opening. This irregularity was located above the retinal pigmented epithelium distorting the inner retinal layers, thereby leading to a loss or disruption of the external limiting membrane and inner segment ellipsoid layers (Fig. 2). The appearance on optical coherence tomography cross section amounted to hyperreflective material, whose volume increased toward the center of the optic nerve head, where it eventually disappeared in the bulk of retinal nerve fiber layer tissue (Figs. 2A to F, Appendix Fig. A1, http://links.lww.com/OPX/A330). Inner retinal layers were compressed above this feature, and the integrity of outer retinal layers might have been compromised (Figs. 2B to E). The area immediately neighboring the protrusion appeared raised (Fig. 2A). Based on the appearance, location, and similarity to features previously reported in children,[12] this

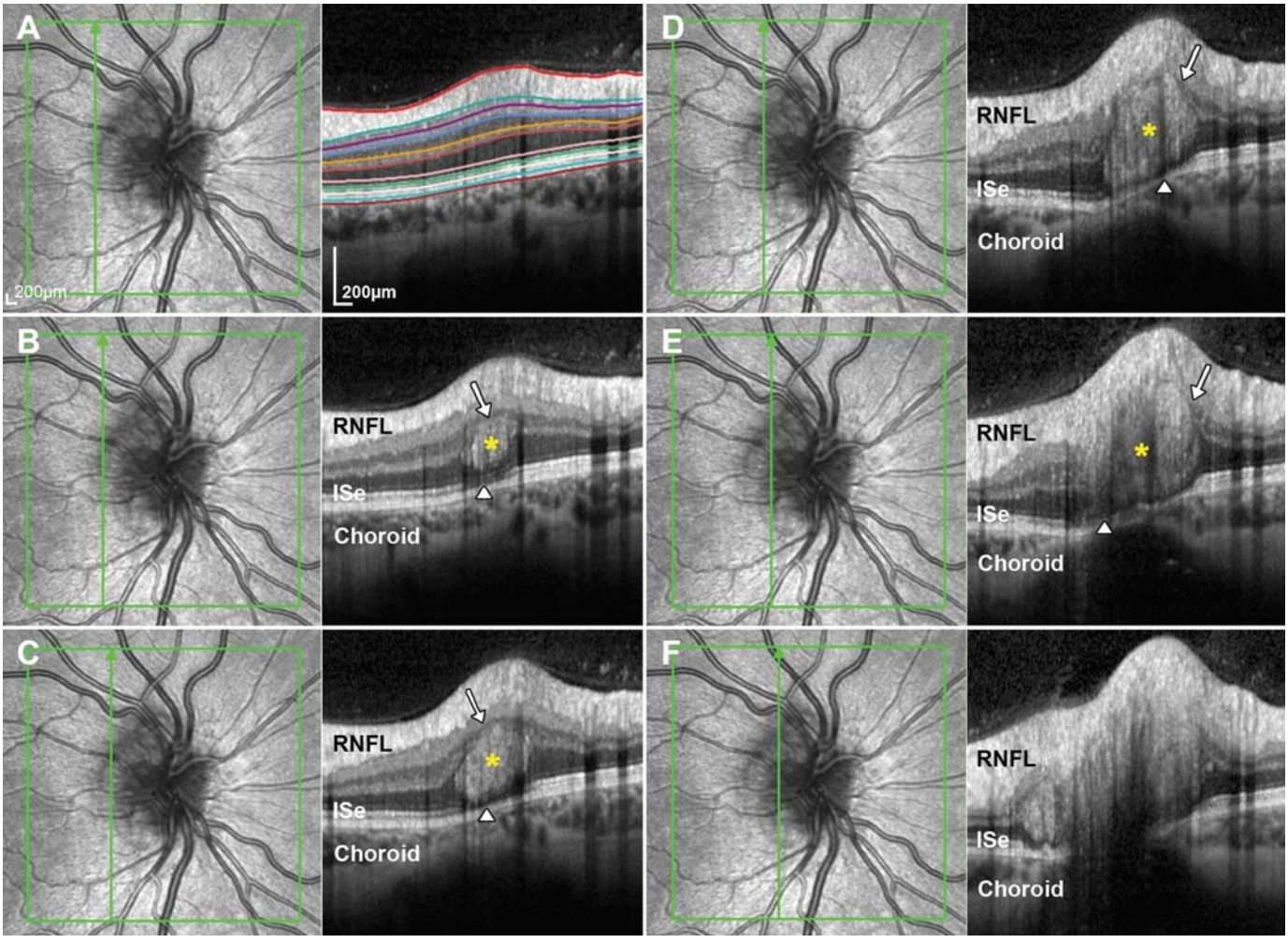

FIGURE 2. Example of RNFL protrusion features observed with spectral domain optical coherence tomography (SD-OCT) scan. Infrared fundus images of a patient's right eye (Table 3, patient 6) showed the appearance of a congenitally heaped (crowded) disc with superior and temporal elevation. Retinal layer segmentation outside the optic disc border appears normal (A). Serial vertical SD-OCT scans every 122 µm through the temporal optic disc border (B through E) reveal a hyperreflective bulge (stars) located within the neurosensory retina leading to a distortion of the inner retinal layers (arrows) and seemingly focal interruption of external bands (arrowheads). The hyperreflective structure eventually connects to the retinal nerve fibers gathering at the optic nerve head (F). (A) Segmentation provided for orientation: (top to bottom) inner limiting membrane (—); RNFL, turquoise line (—); ganglion cell layer, purple line (—); inner plexiform layer, blue line (—); inner nuclear layer, orange line (—); outer plexiform layer, rose line (—); outer nuclear layer, external limiting membrane (—); myoid zone of the photoreceptors, inner segment ellipsoid zone (ISe; —); photoreceptor outer segments, cone interdigitation with RPE (—); RPE (—); RPE/Bruch's membrane complex (—), choroid.

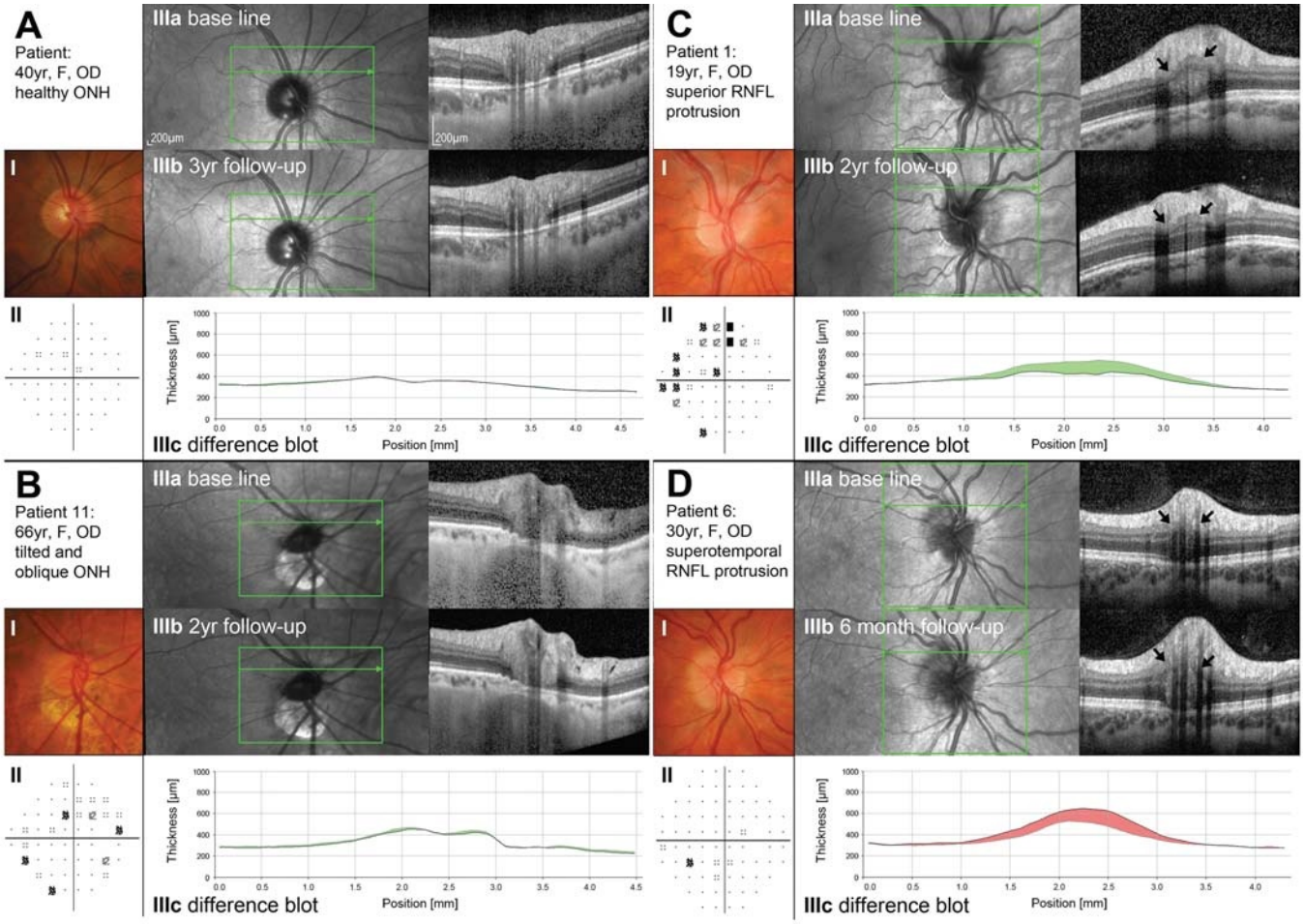

FIGURE 3. Progression of RNFL protrusion (C, D) in comparison to normal and tilted, oblique discs. (A, B) The convergence of RNFL at the optic nerve head (ONH) is accompanied by a disruption of the retinal layers and thinning of the underlying choroid as demonstrated from a normal, healthy optic disc (A). The same principle applies in patients with tilted and/or oblique optic discs, which can display a number of associated features, such as parapapillary atrophy and widespread field defects seen in patient 11 (B, Appendix Table A1, http://links.lww.com/OPX/A329). Note that the retinal thickness in both (A) and (B) remained stable over the follow-up period. (C, D) Retinal nerve fiber layer protrusion is distinguished from the normal entry of RNFL into the ONH by a separation and distortion of inner retinal layers (arrows) leading to a focal disruption of the neurosensory retina. Follow-up on two patients suggested that this protrusion can either diminish (C, patient 1) or further expand (D, patient 6). I: Fundus photography of the ONH; II: Pattern deviation of the patient's visual field tests; III: Characteristic OCT B-scans superior of the patient's ONH at baseline (IIIa), follow-up (IIIb), and the resulting change in total retinal thickness (IIIc, green represents a decrease and red an increase in total retinal thickness).

anomaly was presumed to be and termed retinal nerve fiber layer protrusion, albeit ultimate proof of its exact nature is still outstanding. This retinal nerve fiber layer protrusion was present in 17 of 66 eyes with tilted discs, bilaterally in seven patients and unilaterally in another three (Table 3), but thus far has not been identified in eyes without disc tilt. Both healthy optic nerve heads (Fig. 3A) and tilted and/or oblique optic discs (Fig. 3B) previously examined at CFEH maintained a stable retinal thickness profile over at least 2 years of follow-up period. On the contrary, patients who were diagnosed as having retinal nerve fiber layer protrusion and available for follow-up displayed changes in the retinal structure (Figs. 3C and D, Appendix Fig. A2, http://links.lww.com/OPX/A331).

Features Associated with Presumed Retinal Nerve Fiber Layer Protrusion

Mean optic disc size for patients with tilted discs was 1.93 ± 0.60 mm^2 (range, 1.06 to 3.38 mm^2), with 35 of 43 patients exhibiting a small disc size (<2.4 mm^2). Discs with retinal nerve fiber layer protrusion appeared firstly to be significantly smaller (n = 9, 1.47 ± 0.41; 1.06 to 2.27 mm^2) than those without (n = 34, 2.06 ± 0.56; 1.13 to 3.38 mm^2; *t* test, $P = .005$). Second, optic discs that feature retinal nerve fiber layer protrusion were more likely to also display elevation (n = 43, $\chi^2(1) = 16.4$, $P < .0001$), with eight patients displaying both retinal nerve fiber layer protrusion and optic disc elevation (Table 3). Third, retinal nerve fiber layer protrusion was more frequently associated with congenitally crowded optic discs (67%) than congenitally (22%) or acquired (11%) tilted discs in comparison to the control group (n = 34), which contained 6% congenitally crowded, 59% congenitally, and 35% acquired tilted optic discs ($\chi^2(2) = 80.4$, $P < .0001$).

Where visual field test results were available (8 patients, 14 eyes), five eyes were affected by localized deficits (paracentral loss, nasal step, quadrantanopia), and another four eyes had diffuse widespread or multiple foci defects (Table 3). It should be noted that all visual field tests from eyes with retinal nerve fiber layer protrusion

were performed with Humphrey Field Analyzer. We did not find any association of the retinal nerve fiber layer protrusion with functional loss (visual acuity [logMAR scale], myopia [spherical equivalent], visual field measurements [mean and pattern deviation], or outcomes) or severity of optic disc tilting (index of tilt and torsion).

DISCUSSION

To date, numerous studies have been conducted to understand the development and clinical implications of tilted discs in healthy and diseased eyes.[15,18,19,23] A previous study on adult tilted optic disc subjects reported a nerve fiber herniation into the protruding Bruch's membrane–choroid complex.[13] We did not observe this postulated true herniation of retinal nerve fiber layer fibers into a subchoroidal space accompanied by superior bending of the protruding tissue in our patients. Another novel finding of nerve fiber bulging was reported in pediatric patients with tilted disc syndrome and proposed as a distinguishing feature between adult and pediatric patients.[12] An identically described retinal nerve fiber layer anomaly was present in some patients with optic nerve head drusen, although no detailed information about the size or tilt in these discs was available.[14] Here, we report a similar observation of a dome-shaped hyperreflective bulge in adult tilted discs, indicative of a misplacement of optic nerve fibers into the neurosensory retinal space. Although histopathologic correlation would be useful to determine the exact composition of this hyperreflective bulge, it may be difficult to obtain. In lieu of such evidence, we cannot exclude for certain that the observed feature constitutes a deposit of unknown nature. Based on the similarity to previous reports[12] and negative outcomes with other imaging modalities, such as B-scan and fundus autofluorescence, this formation is most likely formed by misplaced nerve fibers.

One could further argue that the described feature may be an artifact resulting from an obliqueness of the optical coherence tomography beam scan angle. This is unlikely considering serial scans of the protrusion were examined, rather than a single optical coherence tomography scan, as well as taking into account features of the protrusion such as defined rounded margins, location within the retinal architecture sparing the hyperreflective retinal nerve fiber layer, and the presence of the protrusion in some cases without elevation. In contrast, blood vessel artifacts show decreased transmission of the optical coherence tomography signal resulting in a vertical linear pattern of posterior shadowing, which is observed to affect all layers of the retina including the choroid. We therefore conclude that this anatomical structure is indeed a protrusion of retinal nerve fibers into the neurosensory retina, significantly associated with parapapillary elevation in tilted discs regardless of age. It should be noted that patients with optic disc pathologies other than tilted optic discs were excluded from the current study, which included those patients diagnosed as having optic nerve head drusen using fundus autofluorescence and B-scan ultrasonography. While both the described retinal nerve fiber layer protrusion and optic nerve head drusen are distinct features, the diagnosis of optic nerve head drusen may incorrectly be made solely from the presence of a hyperreflective bulge on optical coherence tomography images.[24,25]

The thickness of retinal nerve fiber layer tissues typically increases, accompanied by a thinning of the choroid, toward the formation of the optic nerve. While the retinal nerve fiber layer may enter the optic nerve at different angles in tilted and/or oblique optic discs, it should generally follow the same pattern. The investigated retinal nerve fiber layer anomaly forces a separation of the neurosensory retina around the area of the outer nuclear layer of varying extension. Whether it qualifies as a herniation, as proposed in conjunction with pediatric tilted disc syndrome,[12] may depend on the definition of breach in confining structures. Our findings suggest that it is not a resounding feature of a tilted optic disc but is frequently present in tilted discs with areas of rim and parapapillary elevation. Such elevation is prevalent in small, crowded optic discs, as well as frequently observed in tilted discs,[6,26] physiologically associated with a loss of cupping due to the convergence of a normal number optic nerve axons at a smaller than average sclera foramen.[27] In this case, convergence occurs at an oblique angle resulting in indistinct margins due to compression and bending of the axons, which can affect varying locations depending on the angle at which the optic nerve enters the globe. It is important to note that it can be rather difficult to differentiate a small elevated optic disc from papilledema; therefore, the presence of retinal nerve fiber layer protrusion may be a differentiating optical coherence tomography feature between the two conditions, although further studies are required to verify this distinction.[28]

Pichi et al.[12] found that patients either remained stable or presented a potential decrease in retinal thickness and spontaneous resolution of the hyperreflective dome-like structure. Unfortunately, 8 of 10 patients originally identified with retinal nerve fiber layer protrusion in this study were lost to follow-up because of the position of CFEH as a referral-only clinic, as well as the fact that the described features were thus far unknown. As such, we have insufficient data to date to draw conclusions regarding longitudinal changes of the observed feature, which may not remain stable over time. Our study indicated that the retinal nerve fiber layer has a high preference to protrude nasally, with involvement in 65% of cases, but was observed at other locations. These findings significantly differed from the initial report, which describes the herniation of the nerve fibers in pediatric tilted disc syndrome nasally only due to bending of the nerve fibers superiorly.[12] Limited number of patients and studies regarding retinal nerve fiber layer protrusion and/or herniation at the optic disc, specifically the lack of longitudinal studies, prevents detailed insights into the pathogenesis of these features to date. The large age range of our cohort nevertheless supports the predominantly congenital nature of tilted discs.[4] Retinal nerve fiber layer protrusion was not associated with sex, parameters of visual acuity and function, or measurements of optic nerve tilt and/or rotation but preferentially occurred in congenitally crowded, tilted, elevated optic discs.

In summary, we describe a characteristic, dome-shaped hyperreflective bulge within the neurosensory retina of adult tilted optic discs, referred to as retinal nerve fiber layer protrusion, which was significantly correlated with rim and parapapillary elevation and can be best detected with the optical coherence tomography B-scan acquired at the elevated aspect. Further investigation to define the natural course and functional significance of retinal nerve fiber layer protrusions is warranted. Histopathologic correlation to determine the exact composition of the hyperreflective bulge would be useful but may be difficult to obtain. Additional studies involving the general population will also be valuable to assess the true prevalence of retinal nerve fiber layer protrusion. Current findings advocate the importance of anatomical features associated with tilted optic discs, which could significantly enhance our understanding of the associated functional deficits. Caution should be undertaken when diagnosing buried optic nerve head drusen based on the presence of a hyperreflective bulge on optical coherence tomography images alone as this feature may be observed in tilted discs.

ARTICLE INFORMATION

Supplemental Digital Content: Appendix Table A1, available at http://links.lww.com/OPX/A329, presents all original data used to differentiate clinical appearance of patients/eyes identified to present with the investigated RNFL abnormality from other patients with tilted optic discs. This includes clinical details for 35 patients (49 eyes) with optic disc tilt b ut without RNFL protrusion, including elevation (E) of the optic disc, spherical equivalent (**SE**) in diopter, visual acuity (**VA**), and main reason for the observed tilt (**R**). Eyes shaded in red were included in statistical analysis.

Appendix Figure A1, available at http://links.lww.com/OPX/A330, provides the reader with clinical data displaying the full extent of the investigated RNFL feature. Horizontal and Vertical serial OCT scans detailing the presentation of the suggested RNFL protrusion using patient #6. The temporal aspect of the RNFL protrusion observed in the right eye of patient #6 is illustrated through seven consecutive line scans (every 122 µm) horizontally (**A**) and vertically (**B**). This is an extension of the information presented in Figure 2, which consists of the first six images of column B. Continuation of the horizontal scans provides details on the temporal protrusion continuing into the optic nerve head and highlights features of the superior protrusion (**C**). The extend of the superior protrusion is illustrated in the continuation of horizontal scans towards the disc rim (**D**). The scan position is indicated on top of each column following the direction of red arrows from top to bottom. Corresponding locations for the temporal and superior protrusion are highlighted by arrow heads in columns A, B and C, D respectively.

Submitted: March 1, 2017

Accepted: September 20, 2017

Funding/Support: This work was supported, in part, by a grant from the National Health and Medical Research Council of Australia (1033224) and Centre for Eye Health, an initiative of UNSW Australia and Guide Dogs NSW/ACT. Guide Dogs NSW/ACT is also a partner on the NHMRC grant and supplemented a PhD scholarship to AL, who also holds an Australian Postgraduate Award. BZ holds a Faculty Research Grant awarded by the School of Optometry and Vision Science, UNSW Australia.

Conflict of Interest Disclosure: None of the authors have reported a conflict of interest.

Author Contributions and Acknowledgments: Investigation: JC, MY, AL; Writing – Original Draft: JC, BZ; Methodology: MY, AL, MK, BZ; Supervision: MH, MY, AL, MK, BZ; Validation: MH, MY, AL; Funding Acquisition: MK, BZ; Formal Analysis: BZ; Writing – Review & Editing: AL, BZ.

The authors thank Paula Katalinic for clinical input and discussions leading up to this project.

REFERENCES

1. How AC, Tan GS, Chan YH, et al. Population Prevalence of Tilted and Torted Optic Discs among an Adult Chinese Population in Singapore: The Tanjong Pagar Study. Arch Ophthalmol 2009;127:894–9.

2. Witmer MT, Margo CE, Drucker M. Tilted Optic Disks. Surv Ophthalmol 2010;55:403–28.

3. You QS, Xu L, Jonas JB. Tilted Optic Discs: The Beijing Eye Study. Eye (Lond) 2008;22:728–9.

4. Apple DJ, Rabb MF, Walsh PM. Congenital Anomalies of the Optic Disc. Surv Ophthalmol 1982;27:3–41.

5. Kim TW, Kim M, Weinreb RN, et al. Optic Disc Change with Incipient Myopia of Childhood. Ophthalmology 2012;119:21–6 e1–3.

6. Park HY, Lee K, Park CK. Optic Disc Torsion Direction Predicts the Location of Glaucomatous Damage in Normal-tension Glaucoma Patients with Myopia. Ophthalmology 2012;119:1844–51.

7. Vongphanit J, Mitchell P, Wang JJ. Population Prevalence of Tilted Optic Disks and the Relationship of This Sign to Refractive Error. Am J Ophthalmol 2002;133:679–85.

8. Park KA, Park SE, Oh SY. Long-term Changes in Refractive Error in Children with Myopic Tilted Optic Disc Compared to Children without Tilted Optic Disc. Invest Ophthalmol Vis Sci 2013;54:7865–70.

9. Grossniklaus HE, Green WR. Pathologic Findings in Pathologic Myopia. Retina 1992;12:127–33.

10. Lee KM, Lee EJ, Kim TW. Lamina Cribrosa Configuration in Tilted Optic Discs with Different Tilt Axes: A New Hypothesis Regarding Optic Disc Tilt and Torsion. Invest Ophthalmol Vis Sci 2015;56:2958–67.

11. Tay E, Seah SK, Chan SP, et al. Optic Disk Ovality as an Index of Tilt and Its Relationship to Myopia and Perimetry. Am J Ophthalmol 2005;139:247–52.

12. Pichi F, Romano S, Villani E, et al. Spectral-domain Optical Coherence Tomography Findings in Pediatric Tilted Disc Syndrome. Graefes Arch Clin Exp Ophthalmol 2014;252:1661–7.

13. Shinohara K, Moriyama M, Shimada N, et al. Analyses of Shape of Eyes and Structure of Optic Nerves in Eyes with Tilted Disc Syndrome by Swept-source Optical Coherence Tomography and Three-dimensional Magnetic Resonance Imaging. Eye (Lond) 2013;27:1233–41.

14. Kulkarni KM, Pasol J, Rosa PR, et al. Differentiating Mild Papilledema and Buried Optic Nerve Head Drusen Using Spectral Domain Optical Coherence Tomography. Ophthalmology 2014;121:959–63.

15. Brito PN, Vieira MP, Falcão MS, et al. Optical Coherence Tomography Study of Peripapillary Retinal Nerve Fiber Layer and Choroidal Thickness in Eyes with Tilted Optic Disc. J Glaucoma 2015;24:45–50.

16. Chung JK, Yoo YC. Correct Calculation Circle Location of Optical Coherence Tomography in Measuring Retinal Nerve Fiber Layer Thickness in Eyes with Myopic Tilted Discs. Invest Ophthalmol Vis Sci 2011;52:7894–900.

17. Hosseini H, Nassiri N, Azarbod P, et al. Measurement of the Optic Disc Vertical Tilt Angle with Spectral-domain Optical Coherence Tomography and Influencing Factors. Am J Ophthalmol 2013;156:737–44.

18. Hwang YH, Yoo C, Kim YY. Myopic Optic Disc Tilt and the Characteristics of Peripapillary Retinal Nerve Fiber Layer Thickness Measured by Spectral-domain Optical Coherence Tomography. J Glaucoma 2012;21:260–5.

19. Law SK, Tamboli DA, Giaconi J, et al. Characterization of Retinal Nerve Fiber Layer in Nonglaucomatous Eyes with Tilted Discs. Arch Ophthalmol 2010;128:141–2.

20. Maruko I, Iida T, Sugano Y, et al. Morphologic Choroidal and Scleral Changes at the Macula in Tilted Disc Syndrome with Staphyloma Using Optical Coherence Tomography. Invest Ophthalmol Vis Sci 2011;52:8763–8.

21. Jamous KF, Kalloniatis M, Hennessy MP, et al. Clinical Model Assisting with the Collaborative Care of Glaucoma Patients and Suspects. Clin Exp Ophthalmol 2015;43:308–19.

22. Keltner JL, Johnson CA, Cello KE, et al. Visual Field Profile of Optic Neuritis: A Final Follow-up Report from the Optic Neuritis Treatment Trial from Baseline through 15 Years. Arch Ophthalmol 2010;128:330–7.

23. Park CY, Kim YT, Kee C. Evaluation of the Influence of Tilt of Optic Disc on the Measurement of Optic Disc Variables Obtained by Optical Coherence Tomography and Confocal Scanning Laser Ophthalmoscopy. J Glaucoma 2005;14:210–4.

24. Lee KM, Woo SJ, Hwang JM. Differentiation of Optic Nerve Head Drusen and Optic Disc Edema with Spectral-domain Optical Coherence Tomography. Ophthalmology 2011;118:971–7.

25. Lee KM, Woo SJ, Hwang JM. Morphologic Characteristics of Optic Nerve Head Drusen on Spectral-domain Optical Coherence Tomography. Am J Ophthalmol 2013;155:1139–47 e1.

26. Samarawickrama C, Mitchell P, Tong L, et al. Myopia-related Optic Disc and Retinal Changes in Adolescent Children from Singapore. Ophthalmology 2011;118:2050–7.

27. Frisén L, Holmegaard L. Spectrum of Optic Nerve Hypoplasia. Br J Ophthalmol 1978;62:7–15.

28. Chiang J, Wong E, Whatham A, et al. The Usefulness of Multimodal Imaging for Differentiating Pseudopapilloedema and True Swelling of the Optic Nerve Head: A Review and Case Series. Clin Exp Optom 2015;98:12–24.